

# THE INFLUENCE OF SPIRAL ARMS ON ACTION-BASED DYNAMICAL MILKY WAY DISK MODELLING

WILMA H. TRICK<sup>1,2</sup>, JO BOVY<sup>3</sup>, ELENA D'ONGHIA<sup>???</sup>, AND HANS-WALTER RIX<sup>1</sup>

*Draft version May 16, 2016*

## ABSTRACT

- One sentence on what RoadMapping is.
- Overall axisymmetric RoadMapping modelling works in the presence of non-axisymmetric spiral arms, as long as the volume is big enough.

*Keywords:* Galaxy: disk — Galaxy: fundamental parameters — Galaxy: kinematics and dynamics — Galaxy: structure — **[TO DO]**

### 1. INTRODUCTION

- Explain what RoadMapping is, also Acronym
- Summarize BR13
- Summarize results of Paper 1, mention that non-axisymmetries were not considered there
- Main question: Does axisymmetric RoadMapping modelling work in the presence of non-axisymmetric spiral arms?
- Consequences: Both potential and orbit DF are not axisymmetric, i.e., the fitted axisymmetric potential model and DF do per se not contain the truth.
- How to approach this: Use simulation by D'Onghia et al. 2013 and apply RM to it
- The potential model we use is chosen mostly for practical reasons and is not necessarily the optimal one for the simulation. Also, we use a single qDF as DF - because it is the simplest thing to do. Also independently of the non-axisymmetries the chosen models might deviate from the truth. Where we investigated deviations between model and truth in isolated test cases, here several assumptions break down simultaneously.
- Explain actions very shortly.  $\mathbf{J} = (J_R, J_\phi = L_z, J_z)$  quantify oscillation in the coordinate directions  $(R, \phi, z)$ . Are calculated from current phase-space position in a given potential  $\Phi$ .
- Say that actions are conserved in an axisymmetric potential, but not in non-axisymmetric potentials. (Maybe the mean vertical action is conserved **[TO DO: Reference]**.) It is therefore important to check, if our modelling works in a system where actions are not conserved.

### 2. RoadMapping MODELLING

#### 2.1. Likelihood

The data that goes into the modelling are the 6D position and velocity coordinates  $(\mathbf{x}_i, \mathbf{v}_i)$  of  $N_*$  stars within the survey volume. For simplicity we use a purely spatial selection function  $\text{sf}(\mathbf{x})$  of spherical shape,

$$\text{sf}(\mathbf{x}) \equiv \begin{cases} 1 & \text{if } |\mathbf{x} - \mathbf{x}_0| \leq r_{\text{max}} \\ 0 & \text{otherwise} \end{cases},$$

whose maximum radius  $r_{\text{max}}$  defines the boundary of the survey volume and which is centred on  $\mathbf{x}_0 \equiv (R_0, \phi_0, z_0 = 0)$ . Given a parametrized potential model  $\Phi(R, z)$  with parameters  $p_\Phi$ , the  $i$ -th star is on an orbit characterized by the orbital actions

$$\mathbf{J}_i \equiv \mathbf{J}(\mathbf{x}_i, \mathbf{v}_i | p_\Phi).$$

The total number of stars being on orbit  $\mathbf{J}_i$  is given by an orbit distribution function  $\text{df}(\mathbf{J})$  with parameters  $p_{\text{df}}$ ,

$$\text{df}(\mathbf{J}_i | p_{\text{df}}) \equiv \text{df}(\mathbf{J}(\mathbf{x}_i, \mathbf{v}_i | p_\Phi) | p_{\text{df}}) \equiv \text{df}(\mathbf{x}_i, \mathbf{v}_i | p_\Phi, p_{\text{df}}),$$

where the latter equivalence arises from the Jacobian determinant between the angle-action coordinates  $(\boldsymbol{\theta}, \mathbf{J})$  and cartesian phase-space coordinates  $(\mathbf{x}, \mathbf{v})$ , which is  $|\partial(\mathbf{x}, \mathbf{v})/\partial(\boldsymbol{\theta}, \mathbf{J})| = 1$  and therefore allows us to treat the  $\text{df}$  equivalently as a distribution of current phase-space coordinates or a distribution of orbital actions only, with uniform distribution in the angles  $\boldsymbol{\theta}$ .

- 
- **Write down likelihood formula**
- **Introduce outlier model as new aspect**
- **Refer to Paper 1 for details how to evaluate it, but mention shortly that it is a combination of nested-grid and MCMC**
- **Mention and reference galpy.**

#### 2.2. Potential and DF model

- Introduce potential model, explain that form of disk was mostly chosen to the closed form expression of  $\Phi$  which allows for fast calculation. Both MNHH, DEHH and KKS pot.

<sup>1</sup> Max-Planck-Institut für Astronomie, Königstuhl 17, D-69117 Heidelberg, Germany

<sup>2</sup> Correspondence should be addressed to trick@mpia.de.

<sup>3</sup> Department of Astronomy and Astrophysics, University of Toronto, 50 St. George Street, Toronto, ON, M5S 3H4, Canada

- Mention action calculation and that we tested explicitly that fixing  $\Delta=0.45$  and using staeckel interpolation grid does not degrade the analysis
- Write down DF formula, simplest DF possible. Others use much more complicated ones.

### 3. DATA FROM A GALAXY SIMULATION

#### 3.1. Description of the galaxy simulation

#### 3.2. Survey volume and data

- Mention that we do not consider any measurement errors

#### 3.3. Symmetrized potential model

#### 3.4. Quantifying influence of spiral arm

### 4. RESULTS

#### 4.1. A single application of RoadMapping

##### 4.1.1. Fiducial test

- $r_{max} = 4kpc$
- $N_* = 20,000$
- MNHH potential

##### 4.1.2. Recovering the stellar distribution

- Figure: (x,y) and (R,z) distribution of residuals of true and best fit stellar distribution. Mark spiral arms as circles with radius  $R_g$ .
- Figure: 1D histograms in R,z,phi, comparison of true, best fit and best fit in symmetrized potential
- Figure: 1D histograms in velocity and different (R,z,phi) bins comparison of true, best fit and best fit in symmetrized potential

##### 4.1.3. Recovering the potential

- Figure: density overview plot
- Figure: vcirc, surfdens overview plot
- Figure: local potential overview plot, scatter plot of stars color coded according to deviation of true

and best fit (maybe also symmetrized) potential. normalize potential such that at solar circle  $\text{pot}=0$ . Both in % of true potential and number of sigma away.

- Figure: forces overview plot, incl. local forces scatter plot
- Discuss somehow that the model parameters are actually themselves not very good recovered. Maybe violin plot?

##### 4.1.4. Recovering the action distribution

- Figure: residuals in action space, comparison of true/symmetrized vs. best fit actions (maybe also true vs. best fit in symmetrized potential), overplot  $L_z = v_{circ} * R_g$  of spiral arms

#### 4.2. Investigation of different aspects

##### 4.2.1. Test suite

- $r_{max} = 1, 2, 3, 4, 5kpc$
- $N_* = 20,000$
- MNHH potential + KKS potential
- $R_{obs} = 5 \text{ and } 8kpc$

##### 4.2.2. Survey volume and choice of potential model

- Figure: x-axis:  $r_{max}$ , y-axis: one panel with mean stellar rms deviation in FR and one with Fz. With different potentials and  $r_{max}$ .

##### 4.2.3. Influence of spiral arms

- Figure: x-axis:  $\langle \kappa \rangle$ , y-axis: one panel with mean stellar rms deviation in FR and one with Fz. Analyses with same potential but at different positions and sizes within the galaxy.
- Figure: x-axis:  $\sigma_{\kappa}$ , y-axis: same as above figure.

### 5. SUMMARY AND CONCLUSION

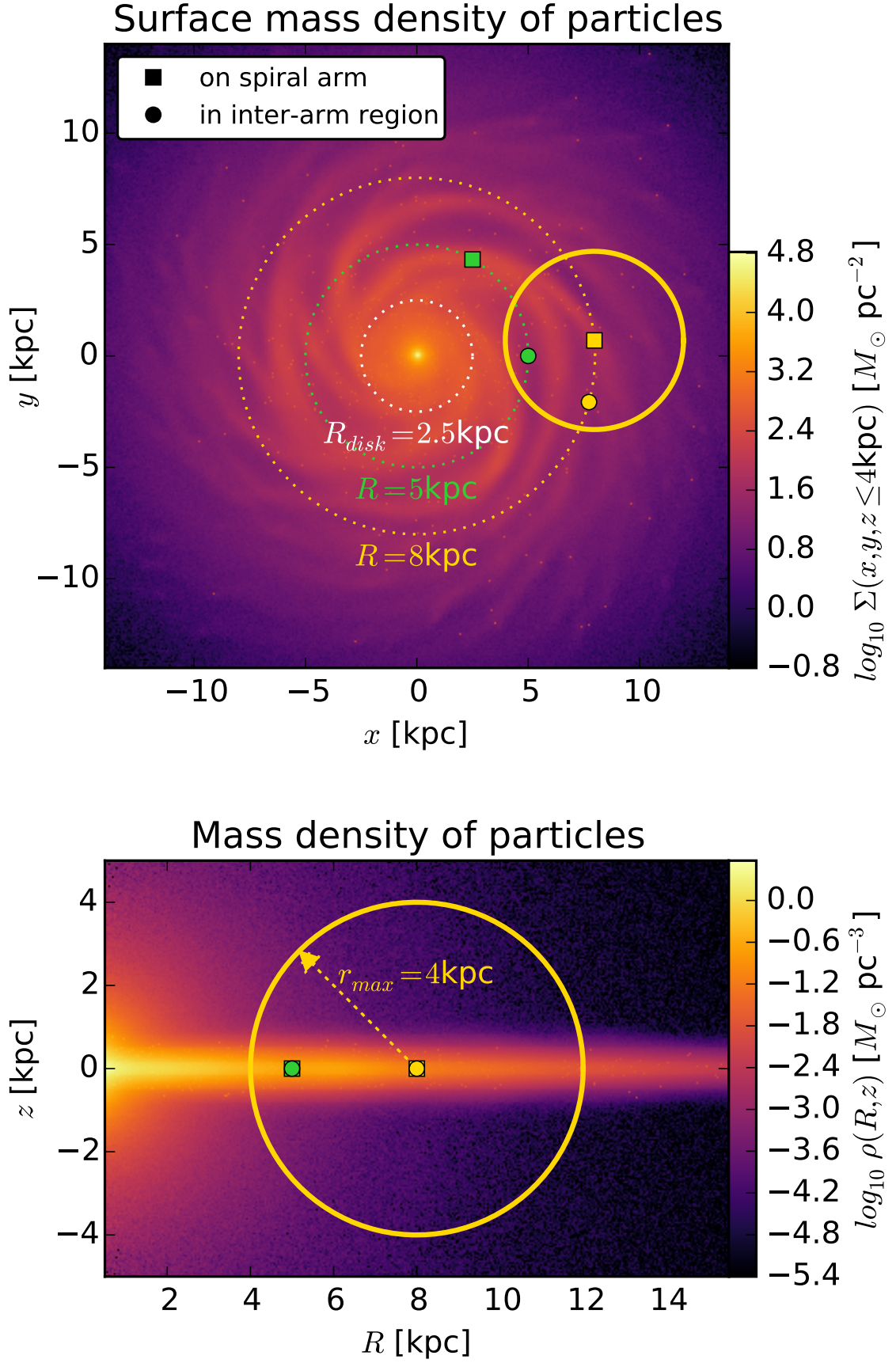
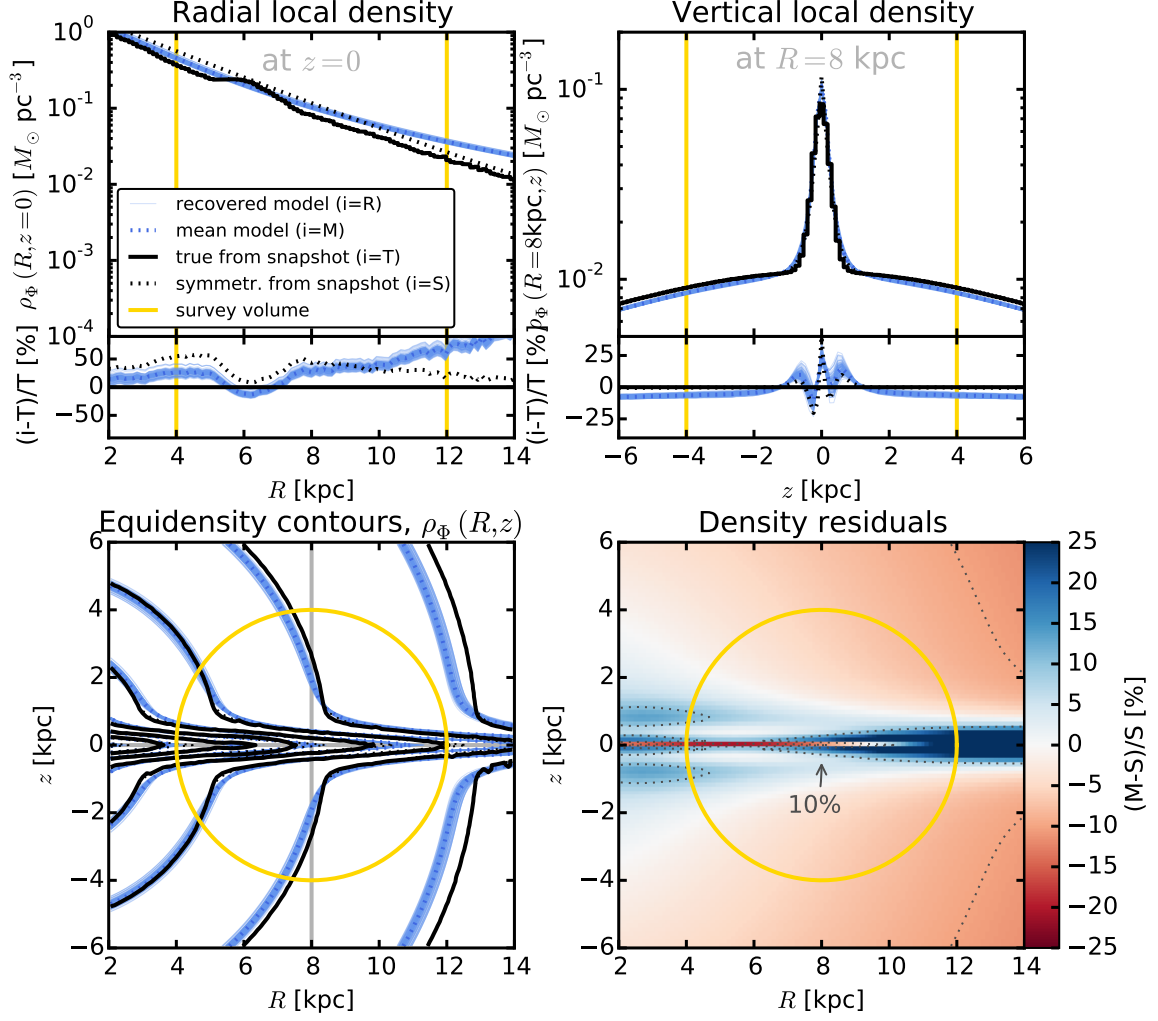
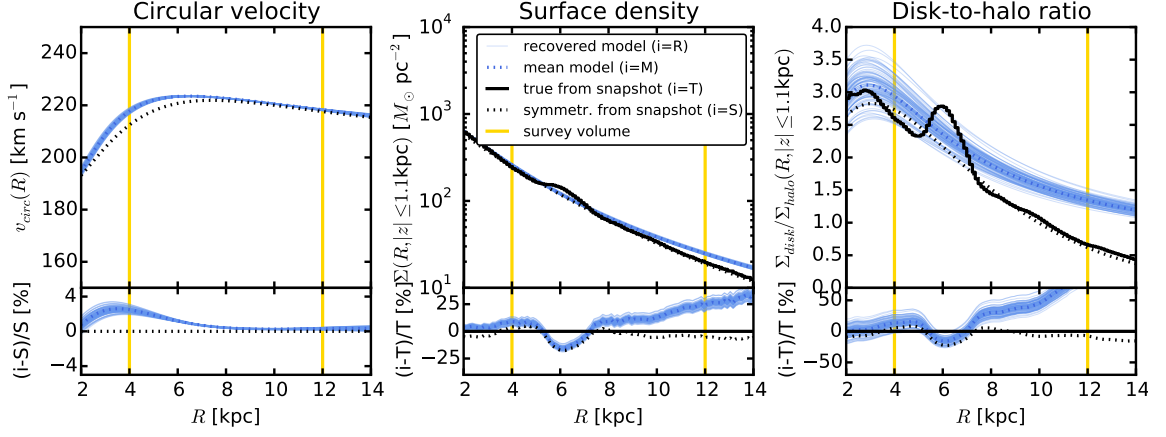


Figure 1.



**Figure 2.** Comparison of the true density distribution  $\rho_{\Phi, T}$  in the galaxy simulation snapshot (solid black line, averaged over  $\phi$ ) with the axisymmetric density distribution  $\rho_{\Phi, R}$  recovered with *RoadMapping* (solid blue lines) from  $N_* = 20,000$  stars in the survey volume with  $r_{\max} = 4$  kpc (yellow line), as described in Section [TO DO]. The first two panels show density profiles along  $(R, z = 0)$  and  $(R = 8 \text{ kpc}, z)$ , together with the relative differences between true and recovered  $\rho_{\Phi}$ . The third panel displays equidensity contours of the matter distribution in the  $(R, z)$  plane. Overplotted are also the symmetrized "true potential's  $\rho_{\Phi, S}$  (dotted black line) (see Section [TO DO]) and the  $\rho_{\Phi, M}$  of the recovered mean model in Table [TO DO] (dotted blue line). The last panel shows the relative difference between the symmetrized "true  $\rho_{\Phi, S}$  and the recovered mean model  $\rho_{\Phi, M}$ . Over wide areas even outside of the survey volume the relative difference is less than 10%. At  $R \gtrsim 8$  kpc and  $z \sim 0$  it becomes apparent that the chosen potential model cannot perfectly capture the structure of the disk. [TO DO: Make sure that this plot actually contains the final analysis and sym. model that I want to show.] [TO DO: Maybe it would be more interesting to see a best fit MNd directly to the potential to see, how well the potential model can actually perform?] [TO DO: Maybe use only stars in the cone that the survey volume probes??]



**Figure 3.** Comparison of the circular velocity curve, surface density profile within  $|z| \leq 1.1$  kpc and disk-to-halo ratio of the surface density along  $R$  for the true potential of the galaxy simulation snapshot (solid black line) and the axisymmetric model potential recovered with *RoadMapping* (solid blue lines) (see Section [TO DO]). Overplotted are also the profiles of the symmetrized "true potential" (dotted black line) (see Section [TO DO]) and the recovered mean model (dotted blue line) (see Table [TO DO]). The circular velocity curve is recovered to less than 5%, especially at larger radii. For the surface density and disk-to-halo ratio *RoadMapping* recovers the truth at radii  $\lesssim 8$  kpc. The deviations at larger radii are connected to the discrepancies in the density in Figure [TO DO]. [TO DO: When I have the force I can probably also calculate the true circular velocity curve!]